Journal of NAMP 72, (2026) 173-186

The Nigerian Association of Mathematical Physics

Journal homepage: https://nampjournals.org.ng

# WELL TEST ANALYSIS OF A HORIZONTAL WELL IN AN INFINITE-ACTING RESERVOIR WITH GAS CAP

**O.U. Orokoh [1] and E. S. Adewole [2]**

[1]*Department of Petroleum Engineering, Federal University of Petroleum Resources, Effurun-Warri, Delta State, Nigeria*

[2]*Department of Petroleum Engineering, University of Benin, Benin City, Edo State, Nigeria.*

ARTICLE INFO

*Article history*:
Received xxxxx
Revised xxxxx
Accepted xxxxx
Available online xxxxx

*Keywords:*
Horizontal well,
Infinite-acting reservoir,
Gas cap,
Dimensionless pressure.

***ABSTRACT***

*Mathematical models have been derived to determine the pressure distribution of a horizontal well in an infinite-acting reservoir with gas cap, using the Source and Green's functions and Newman's product rule. The dimensionless pressure, $P_D$ increases with time and then plateaus signifying the effects of gas cap. The dimensionless pressure derivative, $P_D$' increases with time and then decreases slowly to zero upon encountering the constant pressure support. In this study, $P_D$ and $P_D$' increase as dimensionless pay thickness, $h_D$ increases, which implies that the smaller the $h_D$ the smaller the $P_D$ and $P_D$' and, for high well productivity, small $h_D$ is required. Also, $h_D$ is the critical factor for extending the life span of a horizontal well completion. This study improves well testing by incorporating vertical and lateral boundary conditions accurately into the models, resulting in reliable mathematical models, and providing insights into well placement strategy and reservoir management.*

## 1. INTRODUCTION

With upsurge in horizontal well technology implementation in oil and gas sector due to its beneficial applications, there is the need to develop analytical models that can evaluate the performance of these horizontal wells and characterize the reservoir surrounding them for viability and economic purpose as horizontal well technology, despite its advantages, is more capital intensive than vertical well technology. Horizontal well technology, for instance, can be applied in unconventional reservoirs, such as shale gas or tight oil formations/thin reservoirs where vertical wells may not be effective, and in complex reservoirs with multiple layers and compartments and is drilled horizontally or at a high angle to access a larger portion of the reservoir, thereby improving recovery rate.

An analytical model will be used here to analyze well test of a horizontal well in an infinite-acting reservoir with gas cap, considering reservoir isotropy.

*Corresponding author: O.U. OROKOH
*E-mail address:* osmondorokoh@yahoo.com
https://doi.org/10.60787/jnamp.vol72no.680

There are existing studies on well test analysis of horizontal well models. Idudje, E. H. et al. [1] did not consider gas cap. Ogbue, M. C. et al [2] considered completely bounded reservoir. Oloro, J. O. et al. [3], Ozka, E. et al. [4,5], Marong, B. L. [6] and Odeh, S.A. et al. [7] utilized source and Green's functions to model horizontal well pressure distribution. Besides, none of the studies provides strategies for elongating life span of horizontal well completion in the reservoir system with gas cap. Hence, the purpose of this study is to address those gaps to investigate the effects of complexity of reservoir isotropy and effects of gas cap on the transient pressure behavior of a horizontal well in an infinite-acting reservoir with gas cap. Strategies for elongating the life span of a horizontal well completion in an infinite-acting reservoir with gas cap will be investigated as well. Relevant type curves will be generated based on dimensionless pressure and pressure derivatives for varying horizontal well designs.

For the reservoir system, an infinite reservoir is a theoretical concept used to describe a reservoir system that behaves as if it extended infinitely in all directions though no reservoir is truly infinite. So, in a horizontal well, once the wellbore storage effects are over, the wellbore pressure transient reflects the pressure transmission out in the reservoir. As time proceeds the response is characteristics of the condition further and further away from the wellbore. At very late times, the pressure response is affected by the influence of reservoir boundaries, but prior to those late times the reservoir response does not 'see' the reservoir boundaries and reservoir acts as if it were infinite in extent. The reservoir system has a special feature, gas cap, at the top. The gas cap is a layer of free gas that accumulates above an oil zone in a reservoir. It can help maintain reservoir pressure, can affect the gas-oil ratio of the produced fluids and can influence the production strategy, such as placement of wells and the management of oil production.

Well test analysis is one of the methods, using mathematical models and scientific knowledge, for assessing horizontal well performance and reservoir characterization.

# 2. METHODOLOGY

The purpose of this work is to investigate the pressure transient behaviour of a horizontal well in an isotropic infinite-acting reservoir bounded vertically by gas cap at the top of the reservoir and sealed at the bottom (with no-flow boundary).

## 2.1 RESERVOIR PHYSICAL MODEL DESCRIPTION

Figure 1 is a physical description of the reservoir with top gas cap and infinite-acting well locations $x_w$, $y_w$ and $z_w$ in x, y and z directions. The reservoir is assumed to be laterally infinitely far away during the flow period. A horizontal well is situated at the center of the reservoir. The length of the well coincides with the x-axis, the width of the well coincides with the y-axis and is considered to be negligible (line source) and the thickness of the reservoir is along z-axis. The well stand-off is $z_w$ away from the bottom of the reservoir to the centre of the well.

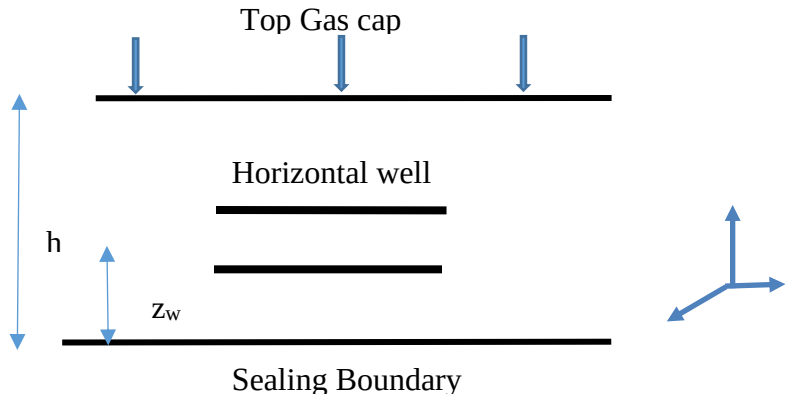


**Figure 1: Reservoir Physical Model**

## 2.2 RESERVOIR MATHEMATICAL MODEL DESCRIPTION

Horizontal well flow in an oil reservoir conforms to the second order linear, heterogeneous partial differential equation called the diffusivity equation which is usually presented in 3-D oil reservoir flow as:

$$\frac{\partial^2 p_D}{\partial x_D^2} + \frac{\partial^2 p_D}{\partial y_D^2} + \frac{\partial^2 p_D}{\partial z_D^2} = \frac{\partial p_D}{\partial t_D} \quad \text{----------(1)}$$

Source and Green's function listed in Gringarten et al. [8] are selected to develop the solution to the partial differential equation 1. The effects of near wellbore skin and wellbore storage are not considered in this study.

**X- axis:** Considering the physical model in Figure 1, the well experiences an infinite slab source from an infinite slab reservoir. Hence, the appropriate source function table is

$$S(x_D, t_D) = \frac{1}{2}\left[\operatorname{erf}\left(\frac{1+x_D}{2\sqrt{t_D}}\right) + \operatorname{erf}\left(\frac{1-x_D}{2\sqrt{t_D}}\right)\right] \text{----------(2)}$$

**Y-axis:** The well is presumed to have an infinite width along the y-axis. That is, infinite plane source in an infinite slab reservoir. The appropriate source function is represented as

$$S(y_D, t_D) = \frac{1}{2\sqrt{\pi t_D}} \exp\left[-\frac{(y_D - y_{wD})^2}{4t_D}\right] \text{----------(3)}$$

**Z-axis**: The top of the reservoir has a special feature, gas cap, which mimics a constant pressure boundary and the bottom is sealed (no-flow boundary). Therefore, along the z-axis, the well experiences an infinite plane source in an infinite slab reservoir. The source function is:

$$S(z_D, t_D) = \frac{2}{h_D}\sum_{n=1}^{\infty} \exp\left(\frac{-(2l-1)^2\pi^2 t_D}{4{h_D}^2}\right) \cos\left(\frac{(2l-1)\pi z_{wD}}{2h_D}\right) \cos\left(\frac{(2l-1)\pi z_D}{2h_D}\right) \quad \text{---(4)}$$

But, according to Newman's product rule in Gringarten et al. [8],

$$P_D = 2\pi h_D \int_0^{tD} S(x_D, \tau).S(y_D, \tau).S(z_D, \tau)\,\partial\tau \text{----------(5)}$$

Putting equations 2, 3, 4 into the equation 5 results in equation 6 as the required dimensionless pressure distribution for a horizontal well in an infinite-acting reservoir with top gas and sealed bottom as follows:

$$P_D = \sqrt{\pi}\int_0^{t_D}\left[\operatorname{erf}\frac{(1+x_D)}{2\sqrt{\tau}} + \operatorname{erf}\frac{(1-x_D)}{2\sqrt{\tau}}\right].\left[\frac{1}{\tau}\exp\left(-\frac{(y_D-y_{wD})^2}{4\tau}\right)\right].\left[\sum_{n=1}^{\infty}\exp\left(\frac{-(2l-1)^2\pi^2\tau}{4{h_D}^2}\right)\cos\left(\frac{(2l-1)\pi z_{wD}}{2h_D}\right)\cos\left(\frac{(2l-1)\pi z_D}{2h_D}\right)\right]d\tau \quad \text{----------(6)}$$

Bourdet, D. [9] gives dimensionless pressure derivative as

$$P'_D = t_D\frac{\partial P_D}{\partial t_D} \quad \text{----------(7)}$$

Applying equation 6 in equation 7, we have

$$P_D{}' = \sqrt{\pi}\left\{\left[\operatorname{erf}\frac{(1+x_D)}{2\sqrt{t_D}} + \operatorname{erf}\frac{(1-x_D)}{2\sqrt{t_D}}\right]\left[\exp\left(-\frac{(y_D-y_{wD})^2}{4t_D}\right)\right]\left[\sum_{n=1}^{\infty}\exp\left(\frac{-(2l-1)^2\pi^2 t_D}{4{h_D}^2}\right)\cos\left(\frac{(2l-1)\pi z_{wD}}{2h_D}\right)\cos\left(\frac{(2l-1)\pi z_D}{2h_D}\right)\right]\right\} \quad \text{----------(8)}$$

## 2.3 COMPUTATION OF WELL RESPONSES

Mathematical models (equations 6 and 8) have been coded in the Python Software and the parameters have been varied severally for sensitivity analysis.

### 2.3.1. Integration via Adaptive Gaussian Quadrature

The integral in equation 6 is evaluated numerically using the **Adaptive Gauss-Kronrod Quadrature** method (specifically the QUADPACK implementation). Unlike standard fixed-point integration, this algorithm dynamically subdivides the integration interval. In the early-time region ($t_D < 0.1$), where the integrand exhibits high-frequency transients and steep gradients, the algorithm increases the density of evaluation points to maintain an absolute error tolerance of $1.49\times10^{-8}$.

### 2.3.2 Infinite Series Convergence and Truncation

The vertical source function accounts for the constant-pressure boundary (gas cap) using an infinite Fourier series. To ensure computational efficiency without sacrificing physical accuracy, an **Exponential Decay Truncation** criterion was applied:

**Summation Limit:** The series is evaluated for n = 1 up to a maximum of 2000 terms.

**Convergence Threshold:** The summation is terminated dynamically when the exponential argument $\exp\left(-\frac{(2n-1)^2\pi^2\tau}{4{h_D}^2}\right)$ falls below -100.
This represents a value of approximately $3.7 \times 10^{-44}$, which is significantly below the machine epsilon for double-precision floating-point numbers. This ensures that the results are exact to the limits of computational precision.

### 2.2.3 Temporal Resolution and Sampling/Time step sizes

To capture the full physics of the reservoir—ranging from initial transient flow to steady-state stabilization—a **Logarithmic Time-Stepping** strategy was employed. Data points were sampled from $t_D = 10^{-4}$ to $10^6$. Logarithmic sampling ensures high resolution during the critical early-time

phase where the pressure derivative ($P_D$') reaches its peak, while avoiding redundant calculations during the late-time plateau where change is negligible.

## RESULTS AND DISCUSSION

The results for horizontal well situated in an infinite-acting reservoir overlaid by gas cap and sealed at the bottom are presented in dimensionless form in table 1 and also in log-log plot in figure 2. Both dimensionless pressure ($P_D$) and dimensionless pressure derivative ($P_D$') increase with time until $P_D$ plateaus from $t_D$=10 while $P_D$' humps between $t_D$=0.01 and 0.1 and decreases and then dives to zero due to effect of a gas cap which mimics a constant pressure boundary. The pressure response is negligible, representing the initial time lag before the reservoir signal reaches the measurement point. At extremely small dimensionless times ($t_D$ = 0.0001), the mathematical "pressure wave" has barely moved a fraction of an inch from the wellbore. During this period, the pressure response is dominated by the expansion or compression of fluid in the wellbore rather than reservoir flow. So, the formulas calculate the pressure change at that specific point and because the response is exponential, and returns an infinitesimal value that is effectively zero.

**Table1: Dimensionless pressure and dimensionless pressure derivative results using these base case parameters - ($x_D$=0.5; $y_D$=0.3; $z_D$=0.5; $h_D$=1; $y_{wD}$=0; $z_{wD}$=0.5 ).**

| $t_D$ | $P_D$ | $P_D'$ |
|---|---|---|
| 0.0001 | 4.260770e-99 | 9.607805e-97 |
| 0.001 | 1.163881e-10 | 2.674587e-09 |
| 0.01 | 2.002051e-01 | 5.267829e-01 |
| 0.1 | 2.845691e+00 | 1.095003e+00 |
| 1 | 4.102668e+00 | 7.238920e-02 |
| 10 | 4.122896e+00 | 5.863330e-12 |
| 100 | 4.122896e+00 | 0.000000e+00 |
| 1000 | 4.122896e+00 | 0.000000e+00 |
| 10000 | 4.122896e+00 | 0.000000e+00 |
| 100000 | 4.122896e+00 | 0.000000e+00 |
| 1000000 | 4.122896e+00 | 0.000000e+00 |

The type curves for the data in table 1 above are presented below as Figure 2.

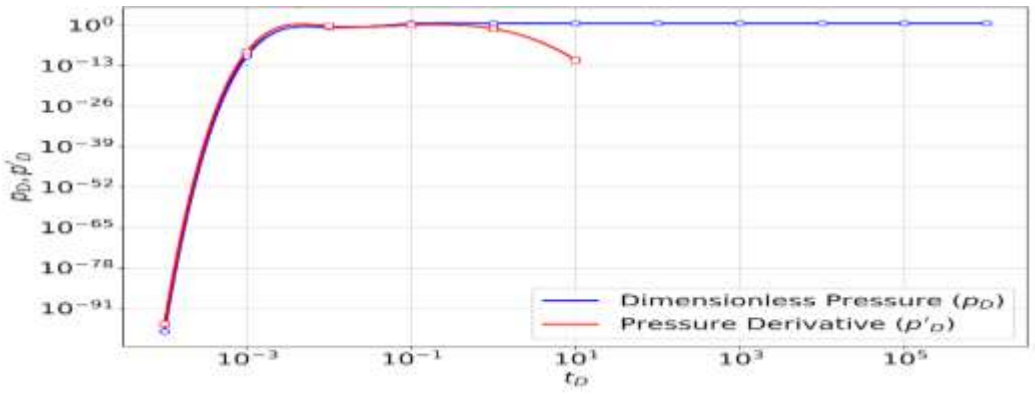


**Figure 2: Diagnostic plot of $P_D$ and $P_D$' vs $t_D$ with result in table 1.**

To determine the slopes and validate the flow regimes, the log-log plot of dimensionless pressure ($P_D$) and its derivative ($P_D$') are analyzed.

**Early-Time Flow Regime: Wellbore Storage**

At the earliest times ($t_D < 10^{-3}$), both the $P_D$ and $P_D'$ curves are essentially coincident and form a straight line; for every log cycle increase in $t_D$, there is an identical log cycle increase in $P_D$. This indicates a unit slope. The unit slope is the classical signature of wellbore storage. During this period, the pressure response is dominated by the expansion or compression of fluid in the wellbore rather than reservoir flow.

**Transition Period: The "Hump"**

Between $t_D = 10^{-3}$ and $t_D = 10^{-1}$, the derivative curve ($P_D'$) deviates from the unit slope, rises to a maximum (a "hump"), and then begins to decline. The slope is continuously changing from +1toward 0. This represents the transition flow period where wellbore storage effects are diminishing and the reservoir starts to influence the pressure response.

**Middle-Time Flow Regime: Infinite Acting Radial Flow (IARF)**

From $t_D \approx 10^{-1}$ to $t_D \approx 10^{1}$, the pressure derivative (PD') flattens out into a horizontal line. A horizontal line on a log-log plot has a zero slope.

**Late-Time Flow Regime: Boundary Effects**

For $t_D > 10^{1}$, the $P_D$ curve reaches a plateau (constant value), and the derivative curve $P_D'$ drops sharply toward zero. $P_D'$ slope is negative and very steep. This behavior indicates a constant pressure boundary (e.g., a massive gas cap). In this regime, the pressure stabilizes as the boundary maintains a constant pressure, causing the derivative to plummet.

**Table 2: Effects of varying $h_D$ on $P_D$ and $P_D$'. Base case parameters ($x_D$= 0.5; $y_D$= 0.3; $z_D$ = 0.5; $z_{wD}$ = 0.5; $y_{wD}$ = 0.0; $h_D$ = 1)**

| $t_D$ | $P_D$ ( $h_D$ = 0.1) | $P_D$' ($h_D$ = 0.1) | $P_D$ ( $h_D$ = 0.5) | $P_D$ '($h_D$ = 0.5) | $P_D$ ($h_D$ = 1) | $P_D$' ($h_D$ = 1) |
|---|---|---|---|---|---|---|
| 0.0001 | 1.731579e-103 | 3.887383e-101 | 8.657894e-103 | 1.943692e-100 | 4.260770e-99 | 9.607805e-97 |
| 0.001 | 4.921191e-16 | 1.084234e-14 | 2.457560e-15 | 5.411766e-14 | 1.163881e-10 | 2.674587e-09 |
| 0.01 | 1.939025e-07 | 3.160158e-07 | 5.638373e-07 | 1.065913e-06 | 2.002051e-01 | 5.267829e-01 |
| 0.1 | 3.577427e-07 | 4.631297e-16 | 2.523480e-06 | 3.669830e-07 | 2.845691e+00 | 1.095003e+00 |
| 1 | 3.577546e-07 | 0.000000e+00 | 2.743528e-06 | 3.510947e-11 | 4.102668e+00 | 7.238920e-02 |
| 10 | 3.577268e-07 | 0.000000e+0 | 2.743534e-06 | 3.147567e-50 | 4.122896e+00 | 5.863330e-12 |

| | | | | | | |
|---|---|---|---|---|---|---|
| 100 | 8.888299e-11 | 0.000000e+00 | 2.743185e-06 | 0.000000e+00 | 4.122896e+00 | 0.000000e+00 |
| 1000 | 8.888299e-11 | 0.000000e+00 | 2.743185e-06 | 0.000000e+00 | 4.122896e+00 | 0.000000e+00 |
| 10000 | 8.888299e-11 | 0.000000e+00 | 2.743185e-06 | 0.000000e+00 | 4.122896e+00 | 0.000000e+00 |
| 100000 | 8.888299e-11 | 0.000000e+00 | 2.743185e-06 | 000000e+00 | 4.122896e+00 | 0.000000e+00 |
| 1e+06 | 8.888299e-11 | 0.000000e+00 | 2.743185e-06 | 0.000000e+00 | 4.122896e+00 | 0.000000e+00 |

**Table 2 Continues.**

| $t_D$ | $P_D$ ($h_D$= 2) | $P_D$' ($h_D$ = 2) | PD ($h_D$= 5) | $P_D$' ($h_D$ = 5) | $P_D$ ($h_D$ = 20) | $P_D$’ ($h_D$ = 20) |
|---|---|---|---|---|---|---|
| 0.0001 | 8.521540e-99 | 1.921561e-96 | 2.130385e-98 | 4.803903e-96 | 8.521460e-98 | 1.921544e-95 |
| 0.001 | 2.327761e-10 | 5.349175e-09 | 5.819403e-10 | 1.337294e-08 | 2.327761e-09 | 5.349175e-08 |
| 0.01 | 4.004103e-01 | 1.053566e+00 | 1.001026e+00 | 2.633914e+00 | 4.004103e+00 | 1.053566e+01 |
| 0.1 | 5.751325e+00 | 2.370774e+00 | 1.437831e+01 | 5.926936e+00 | 5.751325e+01 | 2.370774e+01 |
| 1 | 9.552566e+00 | 7.888885e-01 | 2.394600e+01 | 2.146384e+00 | 9.578398e+01 | 8.585538e+00 |
| 10 | 1.007026e+01 | 1.106455e-03 | 2.610767e+01 | 2.260732e-01 | 1.045118e+02 | 1.095770e+00 |
| 100 | 1.007041e+01 | 2.633442e-28 | 2.621810e+01 | 9.996596e-06 | 1.053987e+02 | 1.083099e-01 |
| 1000 | 1.007041e+01 | 0.000000e+00 | 2.621810e+01 | 7.809377e-45 | 1.053987e+02 | 1.316043e-04 |
| 10000 | 1.007041e+01 | 0.000000e+00 | 2.621810e+01 | 0.000000e+00 | 1.053987e+02 | 3.086048e-29 |
| 100000 | 1.007041e+01 | 0.000000e+00 | 2.621810e+01 | 0.000000e+00 | 1.053987e+02 | 0.000000e+00 |

| | | | | | | |
|---|---|---|---|---|---|---|
| 1e+06 | 1.007041e+01 | 0.000000e+00 | 2.621810e+01 | 0.000000e+00 | 1.053987e+02 | 0.000000e+00 |

The figure 3 below shows graphical relationship between $P_D$ and $P_D$' responses for various $h_D$:

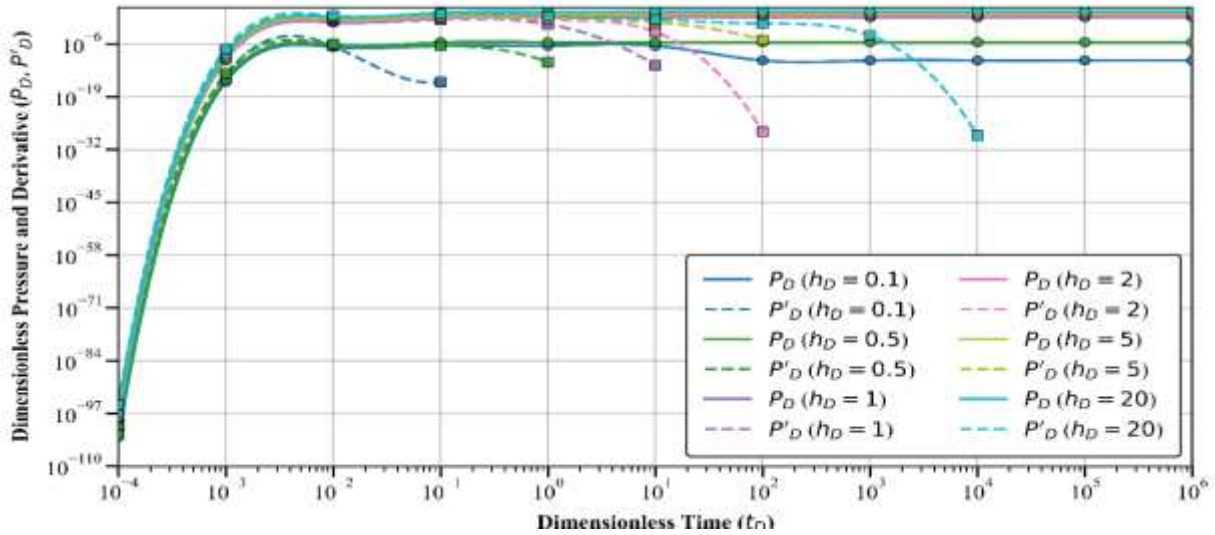


**Figure 3: Plot showing $P_D$ and $P_D$' vs $t_D$ for various $h_D$ (0.1, 0.5, 1, 2, 5, 20)**

The dimensionless reservoir thickness ($h_D$) influences the pressure response, $P_D$ and $P_D$' in a system with a constant-pressure boundary as shown in table 2. The system exhibits a clear transition from a transient phase to a steady-state flow regime. There is a direct non-linear relationship. As $h_D$ increases, the total drawdown required to maintain flow increases significantly. It is observed that for large $h_D$(20 to 1), the stabilized pressure and peak derivatives are proportional to $h_D$. For example, $P_D$ at $h_D$ =20 is roughly 4 times larger than at $h_D$ =5, and 25 times larger than at $h_D$ =1.

Then for small $h_D$ (0.5 to 0.1), once $h_D$ drops below 1, the observed pressure drawdown becomes nearly negligible ($10^{-6}$ to $10^{-11}$ range). This suggests that for very thin reservoirs (relative to the wellbore or distance to the boundary), the system provides almost no resistance to flow from the constant-pressure source.

These results describe a reservoir model where $h_D$ dictates the pressure drop for production. A high $h_D$ represents a more restricted or thicker reservoir flow path requiring higher drawdown. When the horizontal well is very long (e.g. $h_D$ = 0.1 or 0.5 cases), the contact area with the reservoir is massive. This results in minimal pressure drawdown to produce at the same rate. The pressure drop to produce is nearly zero, because the well is so efficient. For shorter well length (high $h_D$), when the well is too short, the flow is more restricted, behaving more like a "point source." This requires a significantly higher pressure drop to maintain production.

**The Impact of Reservoir Thickness ($h_D$) on Breakthrough Time**

The data in table 3 data set shows that $h_D$ is the most critical factor in delaying the influence of the gas cap. Breakthrough occurs much earlier in thinner reservoirs. For $h_D$ =1, the derivative $P_D$' drops to near zero ($5.86\times 10^{-12}$) by $t_D$ = 10.

In thicker reservoirs, the transient flow period is significantly extended. For $h_D$ = 20, the derivative is still substantial (1.09) at $t_D$ = 10 and does not drop to near-zero levels until $t_D$ = 10,000. To elongate completion life, the well should be placed in the thickest possible section of the oil column, maximizing the vertical distance between the lateral and the gas-oil contact, because the highest $h_D$ keeps the well in transient flow state much longer (makes the well take much more time to reach steady state flow).

**Table 3: Effects of varying $y_{wD}$ on $P_D$ and $P_D$' with three sets of parameters below:**

**Base case parameters: ($z_{wD}$=0.5;$z_D$ =0.5; $h_D$=1; $y_D$=0.3; $y_{wD}$=0; $x_D$=0.5)**

| $t_D$ | $p_D$ @ ($y_{wD}$ = 0.1) | $p_D$' @ ($y_{wD}$= 0.1) | $p_D$@ $y_{wD}$ = 0.2) | $p_D$' @ ($y_{wD}$ = 0.2) | $p_D$ @ ($y_{wD}$ =0.8 | $p_D$ '@ ($y_{wD}$ =0.8 ) |
|---|---|---|---|---|---|---|
| 0.0001 | 1.850502e-44 | 1.859664e-42 | 2.724528e-11 | 6.942575e-10 | 2.981869e-273 | 1.840058e-270 |
| 0.001 | 6.861752e-05 | 7.176915e-04 | 4.491791e-01 | 1.297617e+00 | 1.803807e-28 | 1.136259e-26 |
| 0.01 | 1.393701e+00 | 1.838653e+00 | 8.497101e+00 | 3.892428e+00 | 1.442170e-03 | 9.648365e-03 |
| 0.1 | 5.647438e+00 | 1.240801e+00 | 1.440723e+01 | 1.337440e+00 | 8.723907e-01 | 7.340026e-01 |
| 1 | 6.990991e+00 | 7.329974e-02 | 1.580622e+01 | 7.385156e-02 | 1.894653e+00 | 6.955078e-02 |
| 10 | 7.011425e+00 | 5.870663e-12 | 1.582677e+01 | 5.875068e-12 | 1.914241e+00 | 5.839923e-12 |
| 100 | 7.011425e+00 | 0.000000e+00 | 1.582677e+01 | 0.000000e+00 | 1.914241e+00 | 0.000000e+00 |
| 1000 | 7.011425e+00 | 0.000000e+00 | 1.582677e+01 | 0.000000e+00 | 1.914241e+00 | 0.000000e+00 |
| 10000 | 7.011425e+00 | 0.000000e+00 | 1.582677e+01 | 0.000000e+00 | 1.914241e+00 | 0.000000e+00 |
| 100000 | 7.011425e+00 | 0.000000e+00 | 1.582677e+01 | 0.000000e+00 | 1.914241e+00 | 0.000000e+00 |
| 1000000 | 7.011425e+00 | 0.000000e+00 | 1.582677e+01 | 0.000000e+00 | 1.914241e+00 | 0.000000e+00 |

Figure 4 is the type curves showing the effects of various $y_{wD}$ on dimensionless pressure and dimensionless pressure derivative with time.

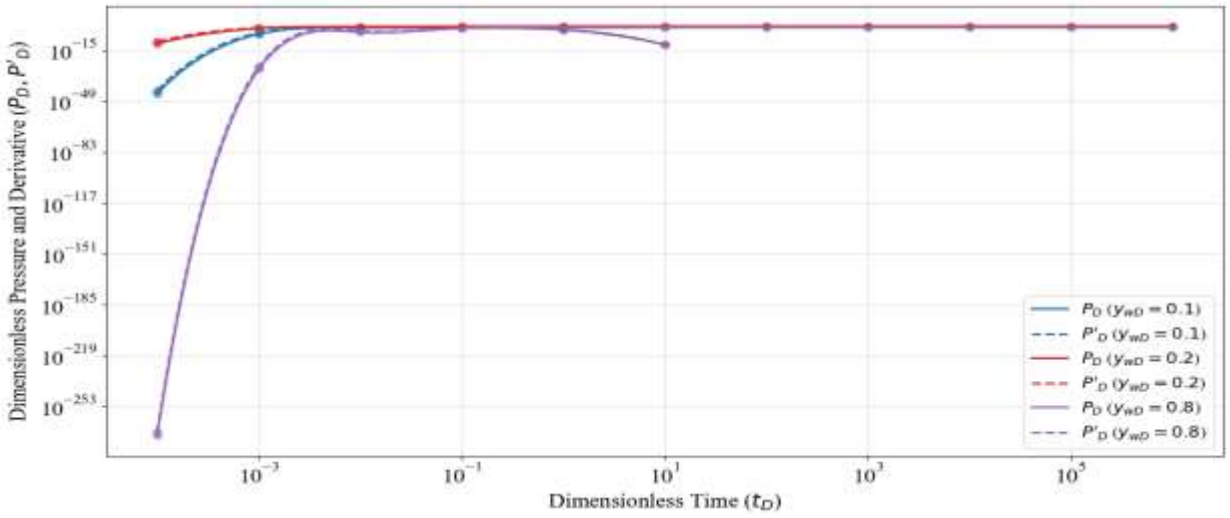


**Figure 4: Diagnostic plot of $P_D$ and $P_D$' v $t_D$ for $y_{wD}$ = 0.1, 0.2, 0.8**

As for the responses of dimensionless pressure and dimensionless pressure derivative evaluated at different dimensionless locations in table 3, $y_{wD}$ = 0.1, 0.2 and 0.8, the value of $y_{wD}$ significantly impacts the magnitude of the pressure drop. At $y_{wD}$ = 0.1, $P_D$ stabilizes at 7.011 and at $y_{wD}$ = 0.8, $P_D$ stabilizes at 1.914 and from the results, it shows that flow experiences the highest resistance at location 0.1, because it is further away from the point of source of pressure support, while at location 0.8 the flow experiences the least resistance to flow, because the well is closer to the constant pressure support. However, it is observed that $P_D$ stabilizes at 1.5827 at location 0.2 at the same time as $P_D$ stabilizes at locations 0.1 and 0.8, which is even smaller than pressure drop at location 0.8. This shows that positioning well at $y_{wD}$ = 0.2 offers least resistance to flow when compared with that of $y_{wD}$ = 0.8 though $y_{wD}$ = 0.2 is further away from constant pressure boundary (gas cap), and this might be as a result of gas coning effect at location 0.8.

**Table 4: Effects of $x_D$ on $P_D$ and $P_D'$. Base case parameters: ($z_{wD}$= 0.5; $z_D$ = 0.5; $h_D$=1; $y_{wD}$= 0; $y_D$ = 0.3)**

| $t_D$ | $P_D$ ($x_D$=0.3) | $P_D'$ ($x_D$=0.3) | $P_D$ ($x_D$=0.4) | $P_D'$ ($x_D$=0.4) | $P_D$ ($x_D$=0.8) | $P_D'$ ($x_D$=0.8) |
|---|---|---|---|---|---|---|
| 0.0001 | 4.260770e-99 | 9.607805e-97 | 4.260770e-99 | 9.607805e-97 | 4.260770e-99 | 9.607805e-97 |
| 0.001 | 1.163881e-10 | 2.674587e-09 | 1.163881e-10 | 2.674587e-09 | 1.163878e-10 | 2.674577e-09 |
| 0.01 | 2.002166e-01 | 5.268899e-01 | 2.002161e-01 | 5.268843e-01 | 1.896841e-01 | 4.854504e-01 |
| 0.1 | 2.930789e+00 | 1.185330e+00 | 2.900088e+00 | 1.147298e+00 | 2.340515e+00 | 8.486858e-01 |
| 1 | 4.289191e+00 | 7.487645e-02 | 4.214004e+00 | 7.377806e-02 | 3.361159e+00 | 6.666313e-02 |
| 10 | 4.309994e+00 | 5.886440e-12 | 4.234554e+00 | 5.876318e-12 | 3.380053e+00 | 5.807377e-12 |
| 100 | 4.309994e+00 | 0.000000e+00 | 4.234554e+00 | 0.000000e+00 | 3.380053e+00 | 0.000000e+00 |

| | | | | | | |
|---|---|---|---|---|---|---|
| 1000 | 4.309994e+00 | 0.000000e+00 | 4.234554e+00 | 0.000000e+00 | 3.380053e+00 | 0.000000e+00 |
| 10000 | 4.309994e+00 | 0.000000e+00 | 4.234554e+00 | 0.000000e+00 | 3.380053e+00 | 0.000000e+00 |
| 100000 | 4.309994e+00 | 0.000000e+00 | 4.234554e+00 | 0.000000e+00 | 3.380053e+00 | 0.000000e+00 |
| 1000000 | 4.309994e+00 | 0.000000e+00 | 4.234554e+00 | 0.000000e+00 | 3.380053e+00 | 0.000000e+00 |

Figure 5 below shows type curves for various $x_D$.

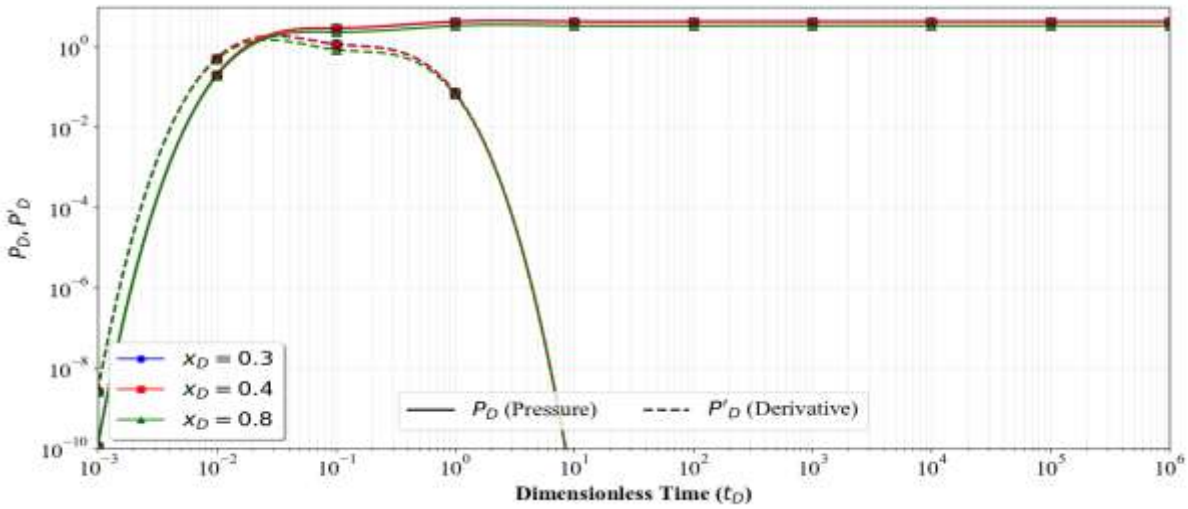


F

**Figure 5: Diagnostic plot of $P_D$ and $P_D$' against $t_D$ for varying $x_D$**

This data that, irrespective of how closer the perforations are to the heel of the well (smaller $x_D$ in this data set), steady-state is reached almost simultaneously (around $t_D$ = 10).

Below are the type curves of $P_D$ and $P_D$' versus $t_D$ for $x_D$=0.25, $y_D$=0.74, $z_D$=0.50, $y_{wD}$=0.0, $z_{wD}$=0.55, $h_D$= 30 and for $x_D$= 0.25, $y_D$= 0.74, $z_D$ = 0.55, $y_{wD}$ = 0.0, $z_{wD}$ = 0.50, $h_D$ = 30.

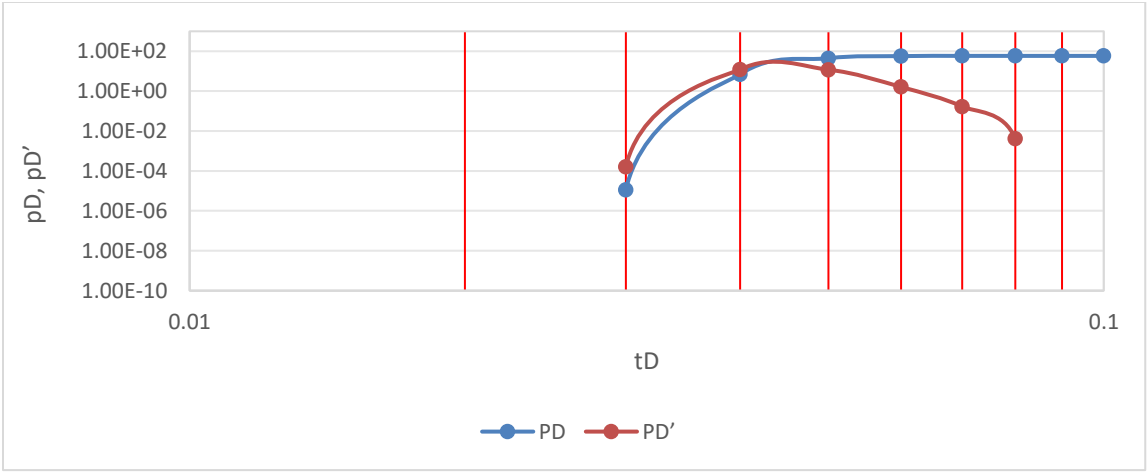


**Figure 6: Type curves of $P_D$ and $P_D$' versus $t_D$ for $x_D$=0.25, $y_D$=0.74, $z_D$=0.50, $y_{wD}$=0.0, $z_{wD}$=0.55, $h_D$= 30 and for $x_D$= 0.25, $y_D$= 0.74, $z_D$ = 0.55, $y_{wD}$ = 0.0, $z_{wD}$ = 0.50, $h_D$ = 30**

Despite the shift in the vertical coordinates of the perforation points, the pressure responses remain identical. The Implication is that placing a horizontal well at $z_{wD}$ = 0.55 provides the exact same drainage efficiency as placing it at $z_{wD}$ = 0.5 or 0.45. Figure 8 shows type curves of $P_D$ and $P_D$' versust $t_D$ for $x_D$ = 0.5, $y_D$ = 0.6, $z_D$ = 0.55, $y_{wD}$ = 0.7, zwD = 0.5, $h_D$=20 and $x_D$ = 0.5, $y_D$ = 0.7, $z_D$ = 0.55, $y_{wD}$ = 0.6, zwD = 0.5, $h_D$ = 20.

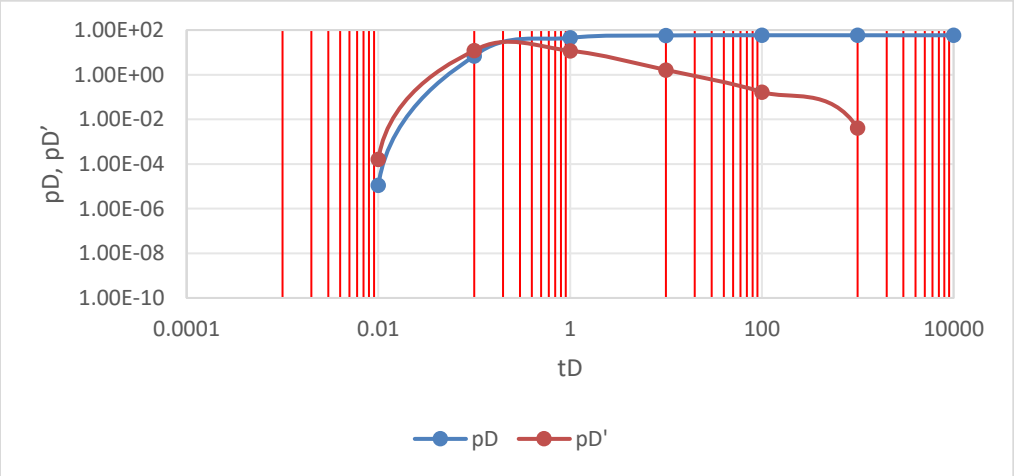


**Figure 7: Type curves of $P_D$ and $P_D$' versust $t_D$ for $x_D$ = 0.5, $y_D$ = 0.6, $z_D$ = 0.55, $y_{wD}$ = 0.7, zwD = 0.5, $h_D$=20 and $x_D$ = 0.5, $y_D$ = 0.7, $z_D$ = 0.55, $y_{wD}$ = 0.6, zwD = 0.5, $h_D$ = 20**

Results in Figures 6 and 7 also show that in reservoir, pressure response at an observation point ($x_D$, $y_D$, $z_D$) due to a source at ($x_{wD}$, $y_{wD}$, $z_{wD}$) is exactly the same as the response that would be measured at ($x_{wD}$, $y_{wD}$, $z_{wD}$) if the source were moved to ($x_D$, $y_D$, $z_D$).

## CONCLUSION

Dimensionless pressure distribution model of a horizontal well in an infinite-acing reservoir bounded vertically by gas cap at the top and sealed vertically at the bottom of the reservoir has been studied. The following conclusions can be drawn from the study:

1) Dimensionless pressure behavior and flow regimes are affected significantly by the constant pressure boundary (gas cap).
2) Dimensionless pressure derivatives exhibit a hump at early flow period.
3) Dimensionless pressures exhibit steady state character when the gas cap is felt during flow.
4) Dimensionless pressure derivative decline to zero the moment dimensionless pressures attain steady state.
5) Infinite-acting flow is extended the larger the lateral extent of the reservoir.
6) Central well location extends the life of the well for all well designs.
7) Early radial flow, transition flow regime and constant pressure behaviour could be observed in this study.
8) The dimensionless well thickness and well length influence well productivity and the time to reach steady state flow period as well.
9) Dimensionless thickness is the critical factor for extending the life span of a horizontal well completion.
10) Perforation positions along the well length axis exhibit almost the same well performance throughout flow period.

**Conflict of interest:** The authors have no conflict of interest.

## REFERENCES


[1] Idudje, E. H., and Adewole, E. S. (2020) "A new test analysis procedure for pressure drawdown test of a horizontal well in an infinite-acting reservoir," *Nigerian Journal of Technology,* 39, 816–820.

[2] Ogbue, M. C., Anamonye, G. U., Aloamaka, A., Agbabi, P. O., Enyi, L. C., Adewole, E. S., and Bello, K. O. (2024) "A comprehensive pressure distribution model for horizontal well in a gas-cap reservoir," *Journal of Science and Technology Research*, 6(2), 1–15.

[3] Oloro, J. O., and Adewole, E. S. (2019) "Derivation of pressure distribution models for horizontal well using source function," *Journal of Applied Science and Environmental Management,* 23(4), 575–583.

[4] Ozkan, E., Raghavan, R., and Joshi, S. D. (1989) "Horizontal well pressure analysis," *SPE Formation Evaluation*, 567–575.

[5] Ozkan, E., and Raghavan, R. (1990) "Performance of horizontal wells subject to bottom water drive," *SPE Reservoir Engineering*, 375–383.

[6] Bakary, L. M., Kiogora, P. R., and Awuor, K. O. (2022) "Well test analysis of a horizontal well in a completely bounded isotropic reservoir," *International Journal of Mathematics Trends and Technology (IJMTT),* 68(8), 46–66.

[7] Odeh, S. A., and Babu, D. K. (1990). "Transient flow behaviour of horizontal wells: Pressure drawdown and buildup analysis," *SPE Formation Evaluation*, 7–15.

[8] Gringarten, A. C., and Ramey, H. J. (1973) "The use of source and Green's functions in solving unsteady state flow in petroleum reservoirs," *Society of Petroleum Engineers Journal,* 13, 285–296.

[9] Bourdet, D. (2002) "Well test analysis: The use of advanced interpretation models," Elsevier, Amsterdam.

[10] Al Rbeawi, S., and Tiab, D. (2013) "Transient pressure analysis of horizontal wells in a multi-boundary system," *American Journal of Engineering Research (AJER)*, 2(4), 44–66.

[11] Horne, R.N. (1995). Modern well test analysis. Petroway Inc., Petaluma, CA.


## NOMENCLATURE

$r_{wD} = \frac{2r_w}{L}$ ; $L_D = \frac{L}{2h}\sqrt{\frac{K}{K_y}}$ ; $h_D = \frac{2h}{L}\sqrt{\frac{K_z}{K}}$ ; $x_D = \frac{2x}{L}\sqrt{\frac{k}{k_x}}$ ; $p_D = \frac{kh\Delta p}{141.2q\mu B}$; $t_D = \frac{0.000264\times 4kt}{\phi\mu c_t L^2}$

B = Formation volume factor, bbl/stb ;
$y_{wD}$ = Dimensionless well coordinate in y-direction;
$x_D$= Dimensionless distance along the x-axis;
$y_D$ = Dimensionless distance along the y-axis;
$z_D$ = Dimensionless distance along the z-axis;
$z_{wD}$ = Dimensionless well coordinate in z-direction;
$P_D$ =Dimensionless Pressure;
$P_D'$= Dimensionless Pressure derivative;
$h_D$= Dimensionless height (pay thickness);
rw = Wellbore radius;
$r_{wD}$ = Dimensionless wellbore radius;
h = Pay thickness;
L = Well length(ft);
$z_w$ = Vertical distance from the bottom boundary to the wellbore (well stand-off)ft;
n = Number of images the series;
$k_x$ = Permeability in x-direction;
$k_y$ = Permeability in y-direction;
$k_z$ = Permeability in z-direction;
$L_D$ = Dimensionless well length;
$\tau$ = Tau(dummy dimensionless time);
$\Phi$ = Porosity(fraction);
$\mu$ = Viscosity(cp);
$c_t$ = Total compressibility(1/psi).